DOI: 10.1002/anie.201409057

Microsolvation

Water–Water and Water–Solute Interactions in Microsolvated Organic Complexes**

*Cristóbal Pérez, Justin L. Neill, Matthew T. Muckle, Daniel P. Zaleski, Isabel Peña, Juan C. Lopez, Jose L. Alonso, and Brooks H. Pate**

***Abstract:** A structural study of microsolvated clusters of β-propiolactone (BPL) formed in a pulsed molecular jet expansion is presented. The rotational spectra of BPL–$(H_2O)_n$ ($n = 1$–5) adducts have been analyzed by broadband microwave spectroscopy. Unambiguous identification of the structures has been achieved using isotopic substitution and experimental measurements of the cluster dipole moment. The observed structures are discussed in terms of the different intermolecular interactions between water molecules and between water and BPL, which include n–π* interactions involving the lone pairs of electrons on water oxygen atoms and the antibonding orbital of the BPL carbonyl group. The changes induced in the structures of the water hydrogen-bonding network by complexation to BPL indicate that water clusters adopt specific configurations to maximize their links to solute molecules.*

Understanding the interactions between organic molecules and water at a molecular level is a central theme in chemistry and biochemistry.[1,2] For biomolecules in their natural aqueous environment, the surrounding water molecules play a critical role in determining molecular structure and biological function. A valuable approach to bridging the gap between gas-phase and solution-phase behavior is to study microsolvated clusters created in supersonic expansion sources, representing the initial steps of the hydration process. This allows water–solute interactions to be probed with high structural sensitivity.

One of the experimental challenges for studies of microsolvated clusters is the generation and detection of species with increasing numbers of attached water molecules. In fact, most studies with rotational resolution (and thus the highest structural sensitivity) involve only one or two water molecules.[3–8] As shown in the formamide study,[4] the most favorable water binding sites can be discovered, but the small number of water molecules involved implies that the molecular behavior is likely still far from that of solution phase. Studies involving more water molecules have been limited thus far to aromatic species such as benzene and phenol, where complexes with seven, eight, and nine water molecules have been probed (but without rotational resolution); in these studies, the solute only weakly perturbs the water hydrogen-bonding structure.[9–13] High-resolution studies of pure water clusters in the gas phase have also been undertaken. The water trimer,[14] tetramer,[15] pentamer,[16] and hexamer[17] were studied by high-resolution terahertz spectroscopy. More recently, using broadband rotational spectroscopy three isomers of the water hexamer, namely cage, prism, and book, were identified and their relative energies determined.[18] The rotational spectra of two isomers of the water heptamer have been also reported[19] as well as the identification of five isomers of the nonamer and four of the decamer.[20]

Herein, we examine the influence that the structure of an organic molecule with multiple water-binding sites has on the formation of its first solvation shell (Figure 1 and Figure 2). The molecule chosen for this study is β-propiolactone (BPL, $C_3O_2H_4$), which can from hydrogen bonds with water at the sites associated with the non-bonding electron pairs of the two oxygen atoms as well as other weaker interactions, such as C−H···O hydrogen bonds and dispersive interactions. BPL is

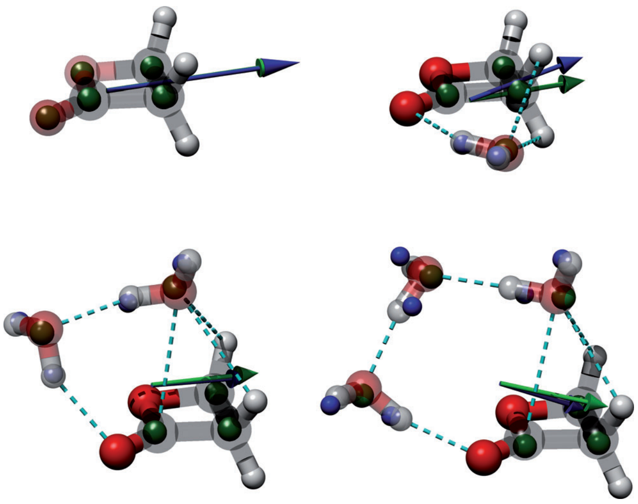

Figure 1. Structures of BPL and its microsolvated complexes BPL–$(H_2O)_n$ ($n = 1$–3). The larger spheres are the ab initio atom positions, calculated at a MP2/6-311++G(d,p) level of theory, while the smaller spheres indicate the experimental r_s atom positions from isotopic substitution. The blue arrow indicates the ab initio dipole moment and the green arrow shows the experimentally derived dipole moment.

---

[*] Dr. C. Pérez, Dr. J. L. Neill, M. T. Muckle, Dr. D. P. Zaleski, Prof. B. H. Pate
Department of Chemistry, University of Virginia
McCormick Road, Charlottesville, VA 22903 (USA)
E-mail: brookspate@virginia.edu
Dr. I. Peña, Prof. J. C. Lopez, Prof. J. L. Alonso
Edificio Quifima Laboratorios de Espectroscopia
y Bioespectroscopia, Parque Cientfico UVa
Universidad de Valladolid, 47011 Valladolid (Spain)

[**] This work was supported by U.S. National Science Foundation (NSF) grants CHE-0960074. Additionally, C.P. and I.P. acknowledge a FPI grant from the Spanish MICINN, grant CTQ2006-05981.

Supporting information for this article is available on the WWW under http://dx.doi.org/10.1002/anie.201409057.

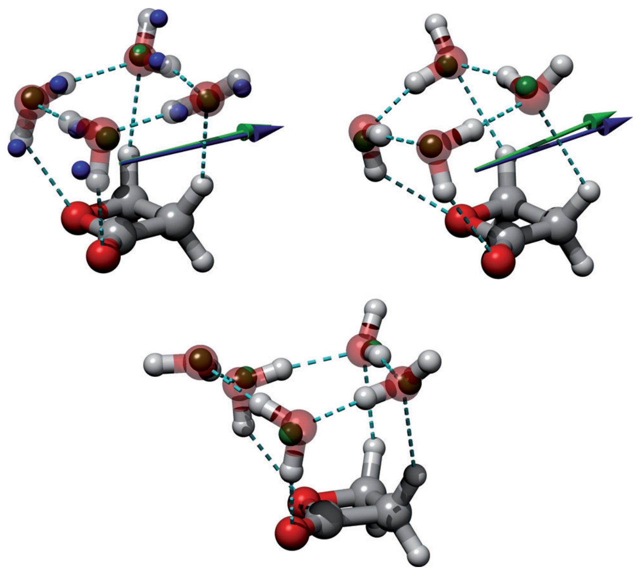

Figure 2. Structures of the microsolvated complexes BPL–$(H_2O)_4$ (top; two isomers) and BPL–$(H_2O)_5$ (bottom). The two BPL–$(H_2O)_4$ isomers have an abundance ratio of approximately 2:1.

itself conformationally rigid and therefore is a good framework for studying the interplay between water–water and solute–water interactions.

We have employed chirped-pulse Fourier transform microwave (CP-FTMW) spectroscopy[19,21] in the 2–18 GHz region to study these complexes (Figure 3). The heavy-atom framework geometry was obtained through the measurement of isotopically labeled species (^{13}C, ^{18}O) as the small changes in mass can be used to determine atom positions, the so-called r_s structure.[22] Further confirmation of the measured structures as well as the hydrogen-bond orientation was performed by measuring the corresponding $(HOD)(H_2O)_{n-1}$ isotopologues. The permanent dipole moments of the complexes were also obtained from Stark effect measurements[23] and are reported in the Supporting Information.

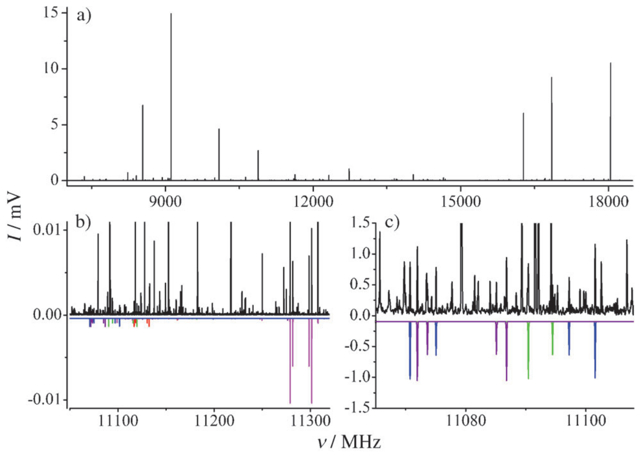

Figure 3. a) The CP-FTMW pulsed-jet spectrum of BPL with a sample of ^{18}O-enriched (10%) water after 2.5 million acquisitions in the time domain with a gate duration of 20 μs. b) Several transitions of the more abundant BPL–$(H_2O)_4$ complex and its corresponding singly-substituted ^{18}O-isotopologue transitions after 1000× magnification compared with 1.5 K simulations (colored traces). c) High resolution view after 10 000× magnification of the transitions belonging to three of those ^{18}O isotopologues of the complex and their simulations (blue, purple, and green traces).

We have measured the rotational spectra and determined structures for BPL–$(H_2O)_n$, $n = 1$–5. We present the ab initio structures of these complexes in Figure 1 (monomer and $n =$ 1–3) and Figure 2 ($n = 4,5$), with the experimentally derived atom positions overlaid (Tables S8-S14 in the Supporting Information). The experimental and calculated dipole-moment directions are also presented in these figures. The deviations between the experimental and calculated atom positions increase as a function of cluster size (Table 1) but the close agreement between the experimental and calculated atom positions and dipole moment provide a clear identification of the clusters.

Table 1: Root-mean-square deviation between calculated and experimental atom positions for BPL and BPL–water complexes.

Species	Deviation [Å]
BPL	0.014
BPL–(H_2O)	0.047
BPL–$(H_2O)_2$	0.107
BPL–$(H_2O)_3$	0.235
BPL–$(H_2O)_4$ (Stronger)	0.110
BPL–$(H_2O)_4$ (Weaker)	0.204
BPL–$(H_2O)_5$	0.244

For each complex, the water molecules form a hydrogen-bonded network which interacts at multiple sites with the BPL molecule. The most favorable water–BPL interaction is an O_{water}–H···$O_{carbonyl}$ hydrogen bond, which is observed in each cluster. In the one-water complex, we observe that the water molecule is located in the symmetry plane (the *a*–*b* principal axis plane) of BPL, and interacts through an O_{water}–H···$O_{carbonyl}$ hydrogen bond and a weaker bifurcated C–H···O_{water} interaction to each hydrogen atom in the adjacent β-methylene group.

In the $n = 2$ complex, one of the water molecules is linked to BPL through an O_{water}–H···$O_{carbonyl}$ hydrogen bond, with the second one sitting above the ring. Interestingly, the oxygen atom of this second water molecule is in a position, with respect to the carbonyl group, that resembles the Bürgi–Dunitz trajectory,[24–26] which describes the most favorable approach of a nucleophile to the carbon of a carbonyl group in an addition reaction. The experimental Bürgi–Dunitz parameters are $R_{O\cdots C} = 3.097(9)$ Å and $\measuredangle(O\cdots C{=}O) = 106(1)°$. The angle formed by the C···O bond and the plane perpendicular to the ring containing the C=O bond is 0.8(2)°. This arrangement is usually interpreted as the existence of a n–π* interaction (Figure 4) in which an electron pair of the nucleophile (H_2O**:**) is delocalized into the π* orbital of the carbonyl group.[26] A natural bond-orbital (NBO) analysis[27] of this complex at the B3LYP/6-311++G(d,p) level of theory further supports the existence of this n–π* interaction, with a stabilization energy of 5 kJ mol^{-1}.

For $n = 3$ (see Figure 1 and Figure 5), the determined r_s positions for the water oxygen atoms show that the water

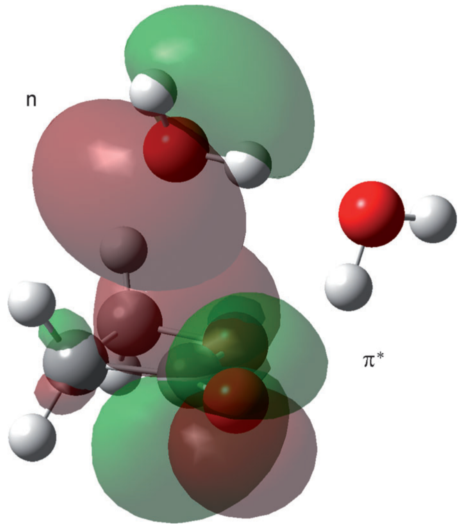

Figure 4. Representation of the n–π* interaction in the BPL–$(H_2O)_2$ complex through a NBO analysis at the B3LYP/6-311++G(d,p) level of theory.

molecules form a chain instead of a cyclical structure as is observed for isolated gas-phase water trimers.[14] The water trimer chain interacts with BPL on both ends in a similar fashion to the BPL–$(H_2O)_2$ complex. Likewise, the position of one of the water molecules, nearly in the plane perpendicular to the ring containing the carbonyl bond and at 3.12(2) Å from the carbonyl carbon atom with an $O_{water}\cdots C{=}O$ angle of 108(1)°, suggests the existence of an n–π* interaction contributing to the stabilization of the observed structure. NBO analysis gives a stabilization energy of 4.09 kJ mol^{-1}. To our knowledge, the $n=2$ and $n=3$ complexes are the first observations of an n–π* interaction in a molecular complex.

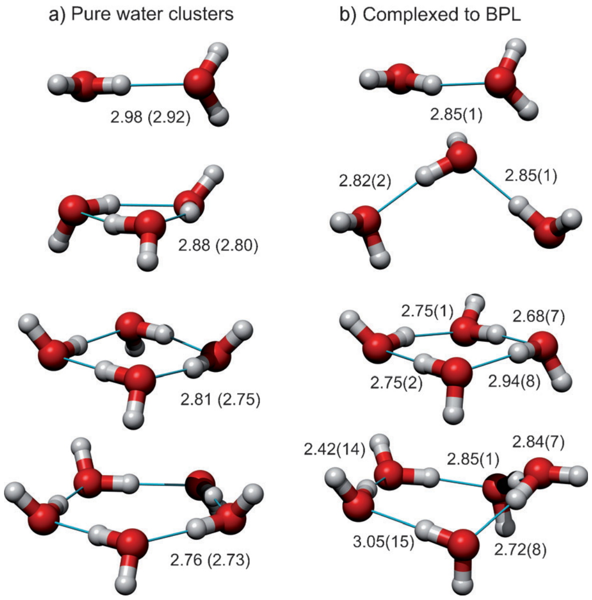

Figure 5. Comparison between a) isolated pure water clusters and b) the observed r_s structures in BPL complexes, showing the lengths of hydrogen-bonding interactions (given in Å). The BPL molecules have been removed from the structures in (b) to aid visualization. For isolated water clusters, experimental O–O distances shown were calculated using the experimentally derived expression $R(n)(O{-}O) = 2.639 + 0.6981\exp(-0.3566n)$, $n=2$–5 from Ref. [16], and ab initio distances for the equilibrium geometry in parentheses from Ref. [30]. Some coordinates of the r_s structures have been fixed to a zero value for distance evaluation (see Supporting Information) and an error of 0.1 Å has been considered.

For $n=4$ and 5, the water molecules arrange into a hydrogen-bonded cyclic structure (Tables S12 and S13). For $n=4$ we observed two different isomeric forms with an abundance ratio of approximately 2:1 (see Figure 2) and a calculated energy difference of 0.2 kJ mol^{-1} at MP2/6-311++G(d,p) level of theory. The two cluster geometries shown in Figure 2 are the two lowest energy structures identified in our computational searches. In each, the water oxygen atoms form a nearly planar ring (dihedral angles of 3.6(1)° for the more abundant isomer and 11(1)° for the less abundant). To further determine the hydrogen-bond geometry, the singly monodeuterated species were measured. Although HOD substitution is not expected to give quantitative structural information because of changes in vibration–rotation contributions to the ground state, it unambiguously reveals the binding sites as well as the orientation of the free hydrogen atoms. As shown in Figure 2 for the more abundant isomer the experimentally determined hydrogen positions reveal how water molecules surrounds the solute.

Although both isomers present an up–up–down–down orientation in the free hydrogen atoms, this is not the minimum-energy orientation for the water tetramer.[15] This configuration is adapted to interact most favorably with BPL through hydrogen bonds. In both, hydrogen bonds are established with the carbonyl group oxygen atom ($O_{water}{-}H\cdots O{=}C$), and to the endocyclic oxygen atom ($O_{water}{-}H\cdots O$). The other two free water hydrogen atoms point away from the BPL atom so that the water oxygen atom lone pairs are offered to the hydrogen atoms of BPL to form weak $C{-}H\cdots O_{water}$ hydrogen bonds. The two complexes differ in the clockwise or anticlockwise arrangement of the endocyclic water–water hydrogen bonds and in the degree of puckering.

In the $n=5$ complex, water molecules form a puckered five-membered ring with intermolecular distances similar to those found in the $n=4$ complexes. Four of the oxygen atoms lie approximately in the same plane, while the remaining atom is out of the plane, puckered away from the BPL ring with a dihedral angle of 147°. The four water molecules with their oxygen atoms in nearly the same plane have a configuration adapted to recognize BPL through hydrogen bonding in the same way as in the $n=4$ complexes; the identified structure has two $O_{water}{-}H\cdots O$ hydrogen bonds from the water network to the BPL carbonyl oxygen atom and to the endocyclic oxygen atom as well as two weak $O_{water}\cdots H{-}C$ bonds. The observed five-water cluster is the lowest-energy structure identified in our computational searches.

Hydrogen-bond cooperativity increases the stability of hydrogen-bonded complexes. Sigma-bond cooperativity is associated with chain or cycles of hydrogen bonds between groups, as hydroxy groups can act simultaneously as hydrogen-bond donors and acceptors.[28] For isolated water complexes, homodromic cycles are the preferred form for clusters with $n > 2$ as in these cases all molecules can act simultaneously as hydrogen-bond donor and acceptor. We detect this behavior also in the BPL–$(H_2O)_4$ and BPL–$(H_2O)_5$ complexes. However, this donor–acceptor role of water is also fulfilled in the case of the complexes with $n = 1$, 2, and 3, where the water molecule or chain forms a cycle with the BPL-solute molecule. The properties of the carbonyl group, which is a stronger Lewis base than water and is capable of withdrawing electron density from the water oxygen atom through n–π* interactions, are also of central importance in the observed structures, especially for the $n = 3$ cluster where the three water molecules prefer to form a chain that closes a cycle with BPL rather than a homodromic cycle.

Our results show that complexation induces measurable structural changes in the $n = 3, 4,$ and 5 complexes. A comparison of the variation in the experimentally derived O−O distances in pure and BPL-complexed water clusters is shown in Figure 5. For $n = 3$, the cyclic ring is broken in favor of a chain water complex, which in the pure $(H_2O)_3$ system is not a stationary point on the potential-energy surface.[29] Cyclic water structures are seen for $n = 4$ and $n = 5$, but are perturbed from those of the pure water clusters. In the $n = 4$ complex, rather than alternating orientations for the protons out of the plane of the water ring (an up–down–up–down configuration), a higher energy (by 3.25 kJ mol^{-1}) isomer (with up–up–down–down configuration) is observed in order to accommodate four water–BPL hydrogen bonds. For $n = 5$, the pure water complex is slightly puckered at its minimum-energy orientation[16,30] and this puckering increases in the BPL–$(H_2O)_5$ complex. In the observed $n = 5$ isomer, the four water oxygen atoms that are involved in direct hydrogen bonds with the BPL unit are nearly in a plane (dihedral angle of < 10°), while the fifth water molecule that is not interacting directly with BPL is puckered by about 20°.

Structural studies of microsolvated BPL in a supersonic expansion provide insight into its most stable water-binding sites and the changes complexation causes to the local water-hydrogen-bonding network. The structures of the observed complexes reflect a trade-off between maximizing the number of BPL–water intermolecular interactions and the minimum-energy structures of the pure water clusters. The resulting structures therefore resemble the pure water complexes, but with significant structural perturbations as a result of water–BPL hydrogen-bonding effects. The extraordinary sensitivity of the rotational spectra of these complexes to small structural changes, and the ability to determine direct structural information and the orientation of the molecular dipole moment with the broadband CP-FTMW spectroscopic technique, provide a useful bridge toward understanding the behavior of molecules in aqueous environments.

Received: September 12, 2014
Revised: October 25, 2014

Keywords: hydrogen bonding · isotopic labeling · microsolvation · microwave spectroscopy · water clusters

[1] P. Ball, *Chem. Rev.* **2008**, *108*, 74–108.
[2] T. Steiner, G. Koellner, *J. Mol. Biol.* **2001**, *305*, 535–557.
[3] J. L. Alonso, E. J. Cocinero, A. Lesarri, M. E. Sanz, J. C. López, *Angew. Chem. Int. Ed.* **2006**, *45*, 3471–3474; *Angew. Chem.* **2006**, *118*, 3551–3554.
[4] S. Blanco, J. C. López, A. Lesarri, J. L. Alonso, *J. Am. Chem. Soc.* **2006**, *128*, 12111–12121.
[5] W. Caminati, J. C. López, S. Blanco, S. Mata, J. L. Alonso, *Phys. Chem. Chem. Phys.* **2010**, *12*, 10230–10234.
[6] J. L. Alonso, I. Peña, M. E. Sanz, V. Vaquero, S. Mata, C. Cabezas, J. C. López, *Chem. Commun.* **2013**, *49*, 3443–3445.
[7] J. Thomas, O. Sukhorukov, W. Jäger, Y. Xu, *Angew. Chem. Int. Ed.* **2014**, *53*, 1156–1159; *Angew. Chem.* **2014**, *126*, 1175–1178.
[8] Q. Gou, G. Feng, L. Evangelisti, W. Caminati, *Angew. Chem. Int. Ed.* **2013**, *52*, 11888–11891; *Angew. Chem.* **2013**, *125*, 12104–12107.
[9] C. J. Gruenloh, J. R. Carney, C. A. Arrington, T. S. Zwier, S. Y. Fredericks, K. D. Jordan, *Science* **1997**, *276*, 1678–1681.
[10] C. J. Gruenloh, J. R. Carney, F. C. Hagemeister, T. S. Zwier, J. T. W. Iii, K. D. Jordan, *J. Chem. Phys.* **2000**, *113*, 2290–2303.
[11] C. Janzen, D. Spangenberg, W. Roth, K. Kleinermanns, *J. Chem. Phys.* **1999**, *110*, 9898–9907.
[12] T. S. Zwier, *Annu. Rev. Phys. Chem.* **1996**, *47*, 205–241.
[13] B. Brutschy, *Chem. Rev.* **2000**, *100*, 3891–3920.
[14] N. Pugliano, R. J. Saykally, *Science* **1992**, *257*, 1937–1940.
[15] J. D. Cruzan, L. B. Braly, K. Liu, M. G. Brown, J. G. Loeser, R. J. Saykally, *Science* **1996**, *271*, 59–62.
[16] K. Liu, M. G. Brown, J. D. Cruzan, R. J. Saykally, *Science* **1996**, *271*, 62–64.
[17] K. Liu, M. G. Brown, C. Carter, R. J. Saykally, J. K. Gregory, D. C. Clary, *Nature* **1996**, *381*, 501–503.
[18] C. Pérez, M. T. Muckle, D. P. Zaleski, N. A. Seifert, B. Temelso, G. C. Shields, Z. Kisiel, B. H. Pate, *Science* **2012**, *336*, 897–901.
[19] C. Pérez, S. Lobsiger, N. A. Seifert, D. P. Zaleski, B. Temelso, G. C. Shields, Z. Kisiel, B. H. Pate, *Chem. Phys. Lett.* **2013**, *571*, 1–15.
[20] C. Pérez, D. P. Zaleski, N. A. Seifert, B. Temelso, G. C. Shields, Z. Kisiel, B. H. Pate, *Angew. Chem. Int. Ed.* **2014**, DOI: 10.1002/anie.201407447; *Angew. Chem.* **2014**, DOI: 10.1002/ange.201407447.
[21] G. G. Brown, B. C. Dian, K. O. Douglass, S. M. Geyer, S. T. Shipman, B. H. Pate, *Rev. Sci. Instrum.* **2008**, *79*, 053103.
[22] J. Kraitchman, *Am. J. Phys.* **1953**, *21*, 17–24.
[23] T. Emilsson, H. S. Gutowsky, G. de Oliveira, C. E. Dykstra, *J. Chem. Phys.* **2000**, *112*, 1287–1294.
[24] H. B. Burgi, J. D. Dunitz, E. Shefter, *J. Am. Chem. Soc.* **1973**, *95*, 5065–5067.
[25] H. B. Burgi, J. D. Dunitz, J. M. Lehn, G. Wipff, *Tetrahedron* **1974**, *30*, 1563–1572.
[26] S. Blanco, J. C. López, S. Mata, J. L. Alonso, *Angew. Chem. Int. Ed.* **2010**, *49*, 9187–9192; *Angew. Chem.* **2010**, *122*, 9373–9378.
[27] A. E. Reed, L. A. Curtiss, F. Weinhold, *Chem. Rev.* **1988**, *88*, 899–926.
[28] L. Evangelisti, W. Caminati, *Phys. Chem. Chem. Phys.* **2010**, *12*, 14433–14441.
[29] O. Mó, M. Yáñez, J. Elguero, *J. Chem. Phys.* **1992**, *97*, 6628–6638.
[30] B. Temelso, K. A. Archer, G. C. Shields, *J. Phys. Chem. A* **2011**, *115*, 12034–12046.